Ref.TH.2877-CERN

IMPORTANT NON-LEADING QCD CORRECTIONS TO $W^{\pm}$ AND Z^{o} PRODUCTION IN HADRONIC COLLISIONS

P. Aurenche and J. Lindfors
CERN - Geneva

A B S T R A C T

We calculate the lowest order QCD corrections to single muon transverse momentum distribution in the process hadron + hadron → $W^{\pm}$ (or Z^{o}) → $\mu^{\pm}$ + anything. Numerical analysis for $\bar{p}p$ collisions at $\sqrt{s}$ = 540 GeV shows the QCD processes to be the dominating production mechanism at $k_T > M_W/2$ and to give a very important correction to the parton model result at and below $k_T = M_W/2$.

Ref.TH.2877-CERN
3 June 1980

The vector bosons $W^{\pm}$ and Z^{o} of the standard $SU(2)\times U(1)$ model are expected to be seen as peaks in the transverse momentum spectrum of single muons produced in hadronic collisions at very high energies [1]. This prediction is based on the assumption of the Drell-Yan production mechanism [2], where quark and antiquark from the incoming hadrons annihilate to form the virtual vector boson, which then decays into two leptons (Fig. 1a). Assuming that the transverse motion of the incoming partons inside the hadrons is negligible, the vector boson is produced at $q_T = 0$, and the high transverse momentum of the observed lepton must be balanced by that of the unobserved lepton (neutrino in the case of $W^{\pm}$). This results into a single muon k_T distribution which is peaked at $k_T = M_W/2$ with a Breit-Wigner fall-off above this value.

However, another type of a production mechanism is provided by the QCD subprocesses, where the vector boson is produced at large q_T with a gluon (or quark) on the opposite side (Fig. 1c,d). Especially one expects these QCD processes to give a large relative contribution above $k_T = M_W/2$.

These two production mechanisms are actually related and non-separable (at least below $k_T = M_W/2$) unless one also observes the opposite side jet typical for the QCD production mechanism. The relation is provided by the factorization theorem [3], which allows one to absorb the mass singularities of the QCD diagrams into the wave functions of the incoming partons. This leading logarithmic QCD effect has been taken into account in several papers [4] by the use of non-scaling quark distributions in the Drell-Yan cross-section. The non-leading QCD contributions, however, have been considered only numerically in a phenomenological quark-mass regularization scheme by Chaichian et al. [5] [see also Halzen and Scott, Ref. 4)].

In this letter we will present in an analytical form the results of our calculation of the non-leading QCD terms. After a brief discussion of the calculation and the conventions used, we take W^{+} production at the future CERN $p\bar{p}$ collider as an example to illustrate the importance of these correction terms. A detailed description of the calculation as well as predictions for different experimentally interesting cross-sections will be given elsewhere.

The calculation was done in the dimensional regularization scheme, where the divergences corresponding to mass and infra-red singularities appear as poles in $\varepsilon = (4-n)/2$. In principle this allows us to present predictions for the physical cross-sections, which are independent of the regularization method, as we can parametrize the Q^2 evolution of the parton distributions using the anomalous

dimensions calculated in the same regularization scheme [6]. We will also give our results for two different definitions of the parton distributions. In the first one (called the BKKU case) the Q^2 evolution is determined by the anomalous dimensions alone [7], the second one (called the AEM case) is defined in deep inelastic scattering by $F_2(x,Q^2) = x\cdot\Sigma e_f^2\cdot q_f(x,Q^2)$ and was used by Altarelli et al. [8]. Furthermore, we choose γ_5 to anticommute with the γ_μ's in n dimensions [see Ref. 9] and the expansion for $Tr[\gamma_\alpha\gamma_\beta\gamma_\delta\gamma_\varepsilon\gamma_5]$ is taken to be the same as in four dimensions. Although the axial part of the QCD matrix elements depends on this prescription, we find that the ambiguous terms do not contribute to the physical cross-section.

With these conventions the basic (Drell-Yan) process gives, at the parton level, the single muon distribution

$$k_0\frac{d\hat{\sigma}^{DY}}{d^3k}(x_1,x_2) = \langle\tfrac{1}{3}\rangle\frac{\alpha^2}{4\sin^4\theta_W}\cdot\frac{1}{2}\cdot\frac{A(x_1^2+x_2^2-\varepsilon)+B(x_2^2-x_1^2)}{(\hat{s}-M^2)^2+(\Gamma M)^2}\,\delta(1-x_1-x_2) \qquad (1)$$

where θ_W is the Weinberg angle and M and Γ are the mass and width of the vector boson ($W^\pm$ or Z^0). The scaling variables x_i (i=1,2) are related to the momentum k of the observed lepton and the momenta p_i (i=1,2) of the incoming partons by $x_i = k_T^2/2p_i\cdot k$ and the squared centre-of-mass energy at the parton level is $\hat{s} = k_T^2/x_1x_2$. The parameters A and B separating the vector and axial parts are given for the process $u(p_1) + \bar{d}(p_2) \to W^+ \to \mu^+\nu_\mu$ by $A = B = 1$.

The parton cross-section from the Compton diagrams of Fig. 1c can be written in the form (here p_1 is the quark and p_2 the gluon momentum)

$$k_0\frac{d\hat{\sigma}^{qg}}{d^3k}(x_1,x_2) = \frac{\alpha_s(\mu^2)}{2\pi}\left[-\frac{1}{\varepsilon}\left(\frac{4\pi e^{-\gamma_E}\mu^2}{k_T^2}\right)^{\varepsilon}\int_0^1 dz\; P_{qg}(z)\,k_0\frac{d\hat{\sigma}^{DY}}{d^3k}\left(x_1,\frac{x_2}{z}\right) + c_{qg}(x_1,x_2)\right] \qquad (2)$$

where $P_{qg}(z) = [z^2+(1-z)^2]/2$ and μ^2 is an arbitrary normalization scale. The first term illustrates the well-known factorization property of QCD mass singularities. Regularizing in the $\overline{MS}$ scheme of Bardeen et al. [6] and choosing $\mu^2 = k_T^2$ leaves only the c_{qg} term as the contribution of the Compton diagrams. For the BKKU case this is the final result to be convoluted with the non-scaling gluon and quark distributions (the scale being k_T^2), but for the AEM case we must substract from c_{qg} terms proportional to $f^g_{AEM}(z) = P_{qg}(z)\cdot\log((1-z)/z) + 3z(1-z)$, which

are calculated in deep inelastic scattering [see Ref. 8)]. Defining $f^{g}_{BKKU}(z) = 0$ we can present the Compton cross-section for the two cases (i = BKKU, AEM) in one formula

$$k_0 \frac{d\hat{\sigma}^{qg,i}}{d^3k}(x_1,x_2) = \langle \tfrac{1}{3} \rangle \frac{\alpha^2}{4\sin^4\theta_w} \cdot \frac{\alpha_s(k_T^2)}{2\pi} \left\{ \frac{A(x_1^2+(1-x_1)^2) + B(1-2x_1)}{2} \cdot \frac{z}{1-x_1} \right.$$

$$\left. \left[\left[P_{qg}^{(z)} \left(\log\frac{1-z}{x_1 z} - \log r - \frac{\hat{s}_0 - M^2}{\Gamma M}\theta \right) + \frac{1}{2} - f_i^q(z) \right] \frac{1}{(\hat{s}_0-M^2)^2+(\Gamma M)^2} + P_{qg}^{(z)} \frac{\theta}{\hat{s}_0 \Gamma M} \right] \right.$$

$$\left. + \frac{A-B}{4} \left[\frac{J}{\hat{s}^2} - \frac{1}{\hat{s}^2}\frac{2}{1-x_1} \left[\left(x_1 + z - 2x_1 z - \frac{M^2}{\hat{s}} \right) \frac{M}{\Gamma}\theta + \left(x_1 + z - 2x_1 z - 2\frac{M^2}{\hat{s}} \right) \log r \right] \right] \right\} \quad (3)$$

where $z = x_2/(1-x_1)$, $\hat{s}_0 = k_T^2/x_1(1-x_1)$ and the functions $\log r$ and θ are defined by [here $\tilde{s} = \hat{s}(x_1+x_2)$]

$$r(x_1,x_2) = \frac{M^2\sqrt{(\tilde{s}-M^2)^2 + (\Gamma M)^2}}{(\hat{s}_0-M^2)^2 + (\Gamma M)^2}$$

$$\theta(x_1,x_2) = \overline{\arctan}\frac{(\tilde{s}-\hat{s}_0)\Gamma M}{(\hat{s}_0-M^2)(\tilde{s}-M^2)+(\Gamma M)^2} + \overline{\arctan}\frac{\hat{s}_0\Gamma}{(\hat{s}_0-M^2)M + \Gamma^2 M}$$

$$+\pi\,\theta\left(\frac{(M^2-\hat{s}_0)(\tilde{s}-s_0)}{(\hat{s}_0-M^2)^2+(\Gamma M)^2} - 1\right) - \pi\,\theta\left(\frac{\hat{s}_0(\hat{s}_0-M^2)}{(\hat{s}_0-M^2)^2+(\Gamma M)^2} - 1\right) \quad (4)$$

Finally the function $J(x_1,x_2)$ can be given in terms of functions r_0 and θ_0 by

$$J(x_1,x_2) = \frac{x_2(1-2x_1-2x_2)}{(x_1+x_2)^2}\left(\log r_0 + \frac{M}{\Gamma}\theta_0\right) - 2\frac{x_2 - x_1(1-x_1-x_2)}{(1-x_1)^2}$$

$$+ \frac{x_1x_2}{x_1+x_2}\left(2 + \frac{x_1(1-x_1)-x_2(1+x_1)}{(x_1+x_2)^2}\right)\left(\frac{\tilde{s}}{k_T^2} + \frac{2M^2}{k_T^2}\log r_0 + \frac{M^3}{k_T^2\Gamma}\theta_0\right)$$

$$r_0 = \sqrt{(\hat{s}-M^2)^2+(\Gamma M)^2}\,/\,M^2 \quad (5)$$

$$\theta_0 = \overline{\arctan}\frac{\tilde{s}-M^2}{\Gamma M} + \overline{\arctan}\frac{\Gamma}{M}$$

The calculation of the annihilation diagrams (Fig. 1d) and of the interference term due to the virtual diagram (Fig. 1b) is more complicated as one must keep terms up to order ε^2 before the cancellation of the infra-red singularity. After a similar procedure as in the Compton case to absorb the mass singularities the sum of the lowest order Drell-Yan and the order α_s annihilation term can be written in the form (i = BKKU,AEM)

$$
\begin{aligned}
k_0 \frac{d\hat{\sigma}^{q\bar{q},i}}{d^3k}(x_1,x_2) = k_0 \frac{d\hat{\sigma}^{DY}}{d^3k}(x_1,x_2)\Bigg\{ & 1 + \left\langle \tfrac{4}{3} \right\rangle \frac{\alpha_s(k_T^2)}{2\pi}\left[\pi^2 - 8 + A_i - \log^2\frac{x_1}{1-x_1} - 3\log x_1(1-x_1)\right]\Bigg\} \\
& + \left\langle \tfrac{1}{3} \right\rangle \frac{\alpha^2}{4\sin^4\theta_W}\,\frac{\alpha_s(k_T^2)}{2\pi}\Bigg\{ \frac{A\left[x_1^2 + (1-x_1)^2\right] + B\left[1-2x_1\right]}{2}\,\frac{z}{1-x_1} \\
& \cdot \Bigg[\Bigg[\frac{1}{(\hat{s}_0 - M^2)^2 + (\Gamma M)^2}\cdot\left[P_{qq}(z)\left(\log\frac{1-z}{x_1 z} - \log r - \frac{\hat{s}_0 - M^2}{\Gamma M}\theta\right) - f_i^q(z) + \frac{4}{3}(1-z)\right] \\
& + \frac{1}{(\hat{s} - M^2)^2 + (\Gamma M)^2}\,\frac{P_{qq}(z)}{z}\left(\log\frac{1-z}{1-x_1} + \log r + \frac{\hat{s} - M^2}{\Gamma M}\theta\right)\Bigg]\Bigg] \\
& + \left\langle \tfrac{4}{3} \right\rangle \frac{A-B}{2}\,\frac{1}{1-x_1}\Bigg[\Bigg[\frac{1-z+2x_1 z}{(\hat{s} - M^2)^2 + (\Gamma M)^2}\left(\log\frac{1-z}{1-x_1} + \log r + \frac{\hat{s} - M^2}{\Gamma M}\theta\right) - \frac{1}{\hat{s}^2}\log r \\
& - \left(1 - z + 2x_1 z + \frac{M^2}{\hat{s}}\right)\frac{\theta}{\hat{s}\,\Gamma M}\Bigg]\Bigg] \\
& + \Bigg[\Bigg[x_1 \leftrightarrow x_2 \;;\; B \leftrightarrow -B \Bigg]\Bigg] \Bigg\}
\end{aligned}
\tag{6}
$$

where the variables z, $\hat{s}$ and $\hat{s}_0$ and the functions $r(x_1,x_2)$ and $\theta(x_1,x_2)$ are the same as in the Compton case. The dependence on the parton distribution definition is now both in the function $f_i^q(z)$ and the constant A_i. For the BKKU case they both vanish, $f^q_{BKKU}(z) = A_{BKKU} = 0$, and for the AEM case they are given by $A_{AEM} = 9 + \frac{2}{3}\pi^2$ and $f^q_{AEM}(z) = P_{qq}(z)\cdot\log((1-z)/z)$ $-\frac{4}{3}\cdot\left[\frac{3}{2}\cdot(1/1-z\big|_+) - 3 - 2z\right]$ with $P_{qq}(z) = \frac{4}{3}\,(1+z^2)/(1-z)\big|_+$.

We note that on the first line of Eq. (6) we have a similar (factorizable) QCD contribution of the form $\left[1+c\cdot\alpha_s\right]\cdot\sigma^{DY}$ as was found for the mass spectrum of lepton pairs in hadronic collisions [8].

The numerical results presented in Figs. 2-4 are for $\bar{p}p$ collisions at $\sqrt{s} = 540$ GeV and at zero rapidity. The Weinberg angle was taken to be $\sin^2\theta_W = 0.23$, which gives $M_W = 77.8$ GeV and $\Gamma_W = 2.47$ GeV (for three quark doublets). A consistent calculation would require the use of parton distributions determined from the deep inelastic scattering data using the appropriate formulae beyond the leading approximation for the BKKU and AEM definitions. However, here we shall take the same Buras-Gaemers type parametrization for the two cases, namely the non-scaling valence quark and gluon distributions of Ref. 9) with $Q^2 = k_T^2$. As the valence distribution does not differ much for the two cases at small x [10], this should be a good approximation for our example.

The Compton contribution (Fig. 2) is important in $\bar{p}p$ collisions only at $k_T > M_W/2$, where one expected the QCD mechanisms to dominate. The Compton term changes sign twice having a remarkable negative peak at $M_W/2$. The annihilation contributions have been presented in Figs. 3a and 3b for the two cases together with the lowest order term so that the $[1+c\cdot\alpha_s]\sigma^{DY}$ part of Eq. (6) is separated from the rest of the annihilation terms. This $c\cdot\alpha_s$ term is about 25% of the lowest order (Drell-Yan) term for the BKKU case and about 90% for the AEM case. For the BKKU case the rest (HO curve) has the same structure as the Compton term, but for the AEM case this term is negative at all $k_T < M_W/2$. Thus there is a large cancellation for the AEM case between the $[1+c\cdot\alpha_s]\sigma^{DY}$ and the HO term. In all cases the non-leading QCD terms have the important negative peak, which smears the peak at $k_T = M_W/2$ predicted by the lowest order Drell-Yan mechanism. The large QCD terms above $k_T = M_W/2$ contribute further to this smearing. The total cross-sections turn out to agree quite well for the two cases (Fig. 4), and the final result is thus independent of the definition of the parton distributions.

These results hold also for single muon production from Z^0 with obvious changes in the couplings. In Fig. 4 we have shown only the Drell-Yan term for Z^0, and we note that the QCD tail from $W^\pm$ production hides the Z^0 peak almost totally. Fortunately Z^0 can be observed also in the mass spectrum of muon pairs [the QCD corrections have been discussed in Ref. 11)].

We conclude that the non-leading QCD terms are very important in the hadronic production of $W^\pm$. They change qualitatively the prediction of the naive parton model and should be regarded as a separate production mechanism above $k_T = M_W/2$. Moreover they increase the total cross-section (integrated over k_T) by a factor of two making thus $W^\pm$ easier to observe in hadronic collisions.

ACKNOWLEDGEMENTS

We thank M.K. Gaillard for reading the manuscript.

REFERENCES

1) R.F. Peierls, T.L. Trueman and L.L. Wang - Phys.Rev. D16 (1977) 1397 ;
C. Quigg - Revs.Modern Phys. 49 (1977) 297 ;
L.B. Okun and M.B. Voloshin - Nuclear Phys. B120 (1977) 459.

2) S.D. Drell and T.M. Yan - Phys.Rev.Letters 25 (1970) 316.

3) R.K. Ellis, H. Georgi, M. Machacek, H.D. Politzer and D. Ross - Phys.Letters 78B (1978) 281 ; Nuclear Phys. B152 (1978) 285 ;
D. Amati, R. Petronzio and G. Veneziano - Nuclear Phys. B140 (1978) 54 ;
A.H. Mueller - Phys.Rev. D18 (1978) 3705.

4) J. Kogut and J. Shigamitsu - Nuclear Phys. B129 (1977) 461 ;
F. Halzen and D.M. Scott - Phys.Letters 78B (1978) 318 ;
I. Hinchliffe and C.H. Llewellyn Smith - Phys.Letters 66B (1977) 281 ; Nuclear Phys. B128 (1977) 93 ;
F.E. Paige - Talk at Topical Conference of New Particles in Super High Energy Collisions, Madison, WI (October 1979) (BNL-Preprint-27066).

5) M. Chaichian and M. Hayashi - Phys.Letters 81B (1979) 53 ;
M. Chaichian, O. Dumbrajs and M. Hayashi - Phys.Rev. D20 (1979) 2873.

6) E.G. Floratos, D.A. Ross and C.T. Sachrajda - Nuclear Phys. B129 (1977) 66 ; B139 (1978) 545 ; B152 (1979) 493 ; Phys.Letters 80B (1979) 269 ;
W.A. Bardeen, A.J. Buras, D.W. Duke and T. Muta - Phys.Rev. D18 (1978) 3998 ;
W.A. Bardeen and A.J. Buras - Phys.Letters 86B (1979) 61 ;
A. Gonzales-Arroyo, C. Lopez and F.J. Yndurain - Nuclear Phys. B153 (1979) 161 ;
A. Gonzales-Arroyo and C. Lopez - CERN Preprint TH. 2734 (1979).

7) L. Baulieu and C. Kounnas - Nuclear Phys. B141 (1978) 423 ;
J. Kodeira and T. Uematsu - Nuclear Phys. B141 (1978) 497.

8) G. Altarelli, R.K. Ellis and G. Martinelli - Nuclear Phys. B157 (1979) 461 ;
J. Kubar-André and F.E. Paige - Phys.Rev. D19 (1979) 221.

9) M. Chanowitz, M. Furman and I. Hinchliffe - LBL Preprint LBL-8855 (1979).

10) A. Białas and A.J. Buras - FERMILAB-PUB 79/73-THY (1979).

11) B. Humpert and W. Van Neerven - CERN Preprint TH. 2834 (1980).

FIGURE CAPTIONS

Figure 1 The Feynman diagrams for the hadronic production of vector boson (dashed line) :
a) the Drell-Yan mechanism $q\bar{q} \to \ell\bar{\ell}$;
b) QCD virtual correction for $q\bar{q} \to \ell\bar{\ell}$;
c) the QCD Compton process $qg \to q + \ell\bar{\ell}$;
d) the QCD annihilation process $q\bar{q} \to g + \ell\bar{\ell}$.

Figure 2 The Compton contribution for the process $\bar{p}p \to W^+ + \text{anything} \to \mu^+ + \text{anything}$ at $\sqrt{s} = 540$ GeV and $y = 0$. The dashed curve is the AEM case and the dash-dotted curve is the BKKU case (the peak is negative). The Drell-Yan contribution (full line) is drawn here and in the following figures to give a common reference curve.

Figure 3 The annihilation contribution for the process $\bar{p}p \to W^+ + \text{anything} \to \mu^+ + \text{anything}$ at $\sqrt{s} = 540$ GeV and $y = 0$. The dashed curve is the factorizable $[1+c\cdot\alpha_s]\sigma^{DY}$ term and the rest of the corrections (denoted by HO) are presented by the dash-dotted curve. The BKKU case is in Fig. 3a and the AEM case in Fig. 3b.

Figure 4 The single muon cross-section to order α_s in QCD for the process $\bar{p}p \to W^+ + \text{anything} \to \mu^+ + \text{anything}$ at $\sqrt{s} = 540$ GeV and $y = 0$. The dashed curve is the AEM case and the dash-dotted curve the BKKU case. The lowest order contribution is presented by a full line both for W^+ and Z^0 production.

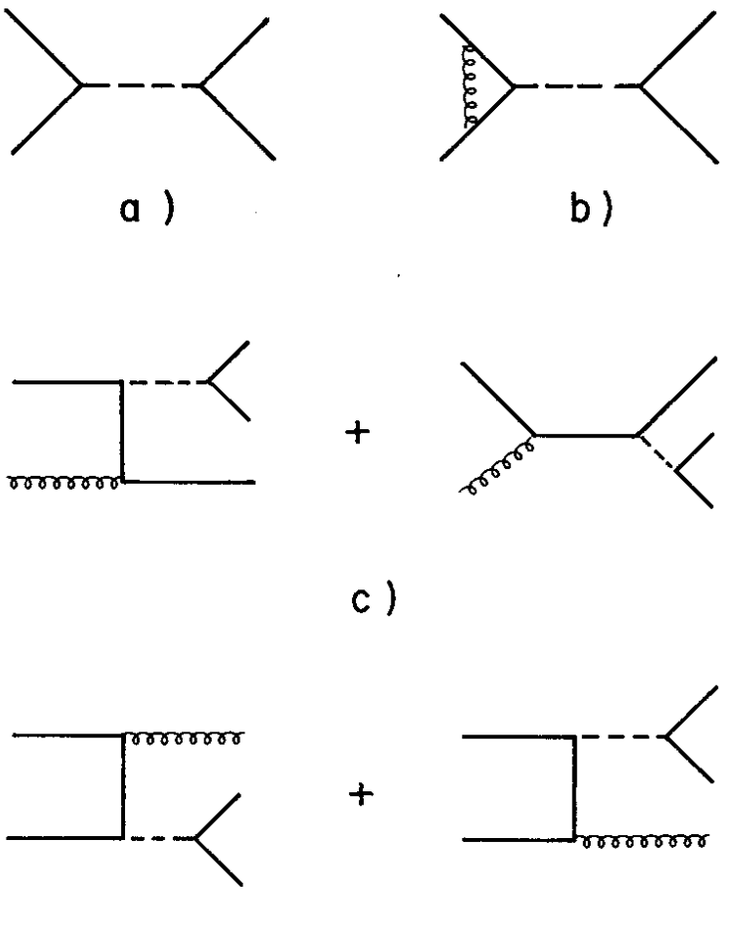

FIG. 1

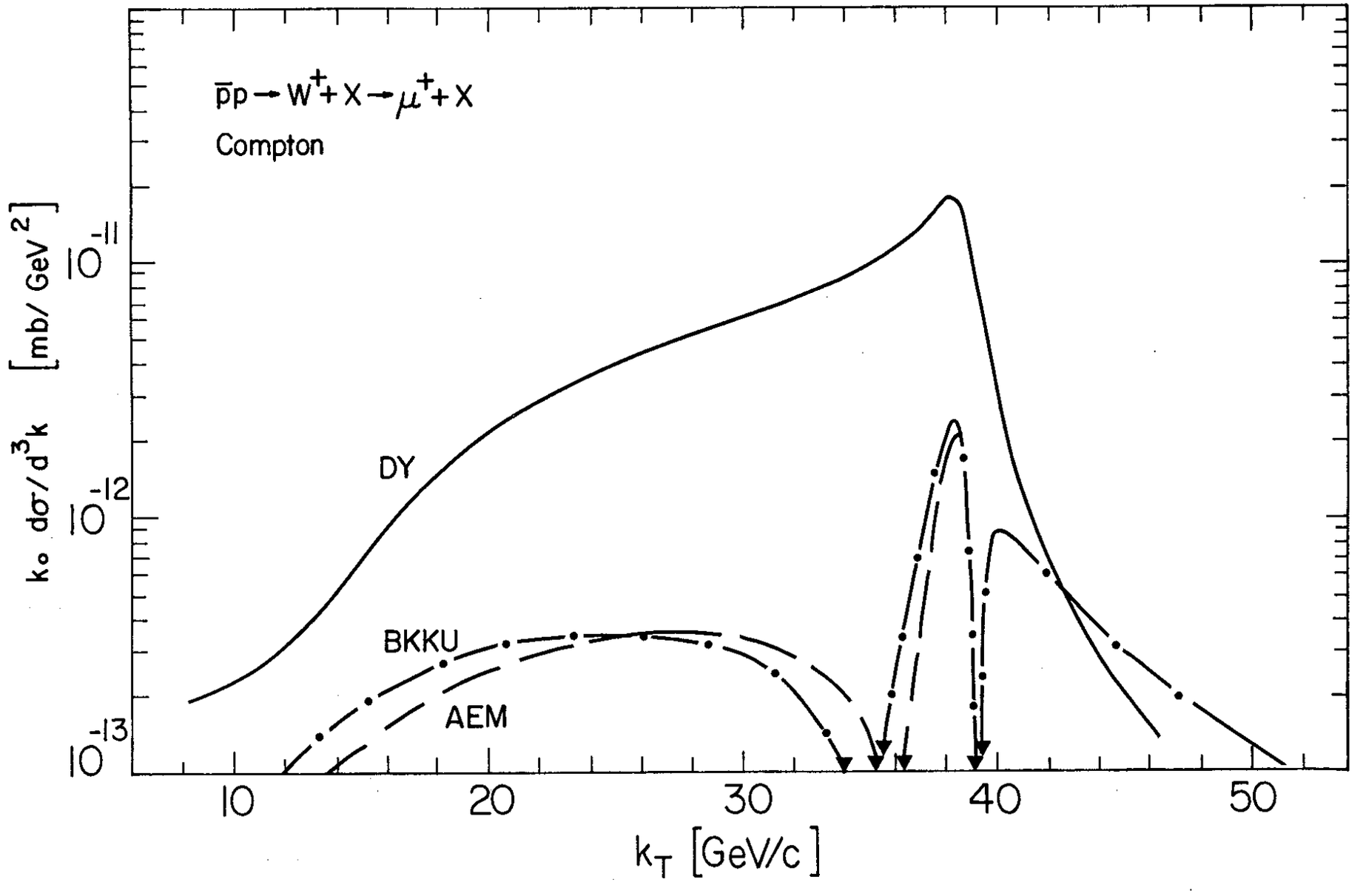
$\bar{p}p \to W^+ + X \to \mu^+ + X$
Compton
DY
BKKU
AEM
$k_0\, d\sigma/d^3k$ [mb/ GeV^2]
10^{-11}
10^{-12}
10^{-13}
10
20
30
40
50
k_T [GeV/c]

FIG. 2

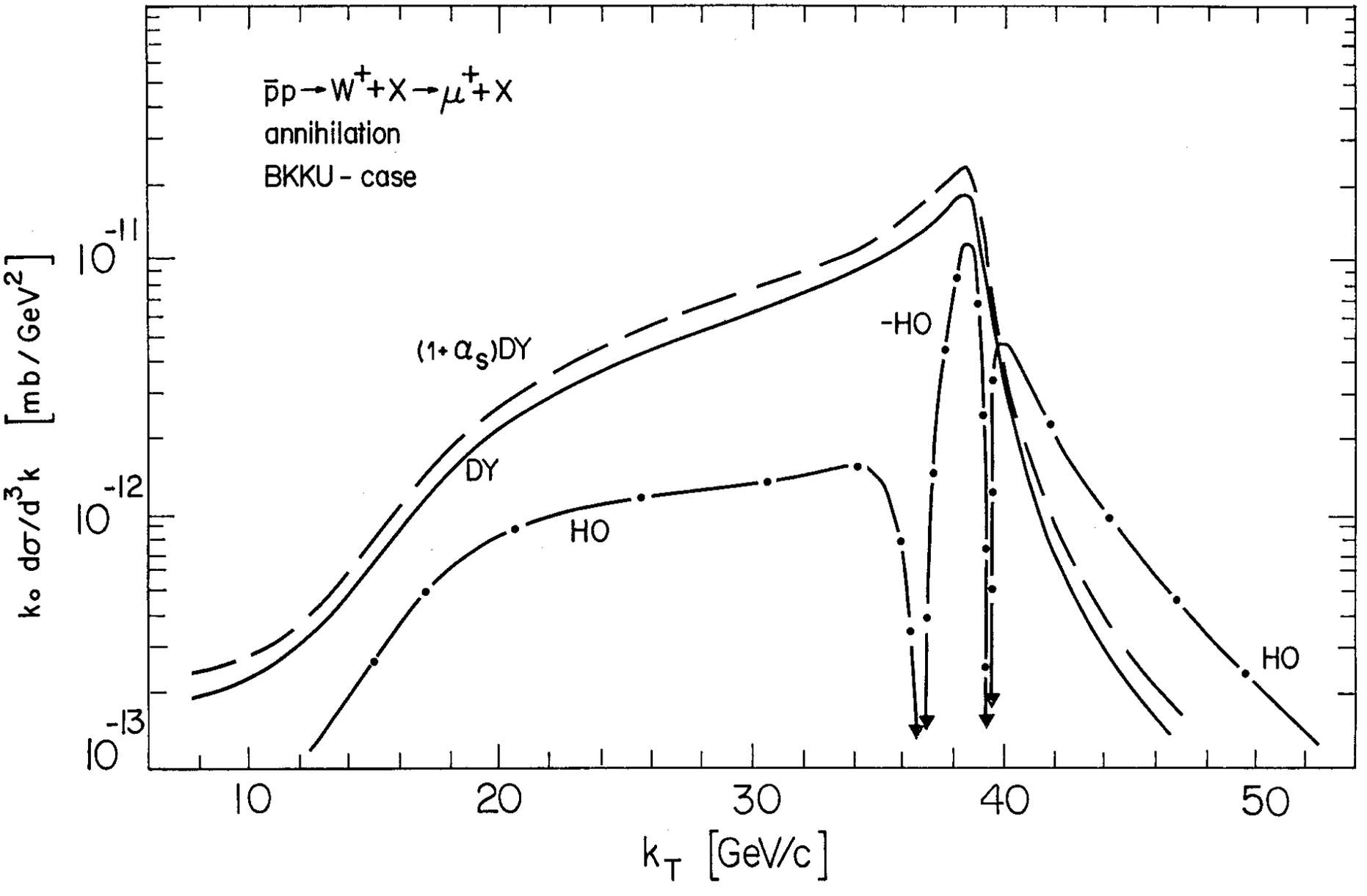
$\bar{p}p \to W^+ + X \to \mu^+ + X$
annihilation
BKKU - case
$(1+\alpha_s)$DY
DY
HO
-HO
HO
10^{-11}
10^{-12}
10^{-13}
$k_0\, d\sigma/d^3k$ [mb/GeV^2]
10
20
30
40
50
k_T [GeV/c]

FIG. 3a

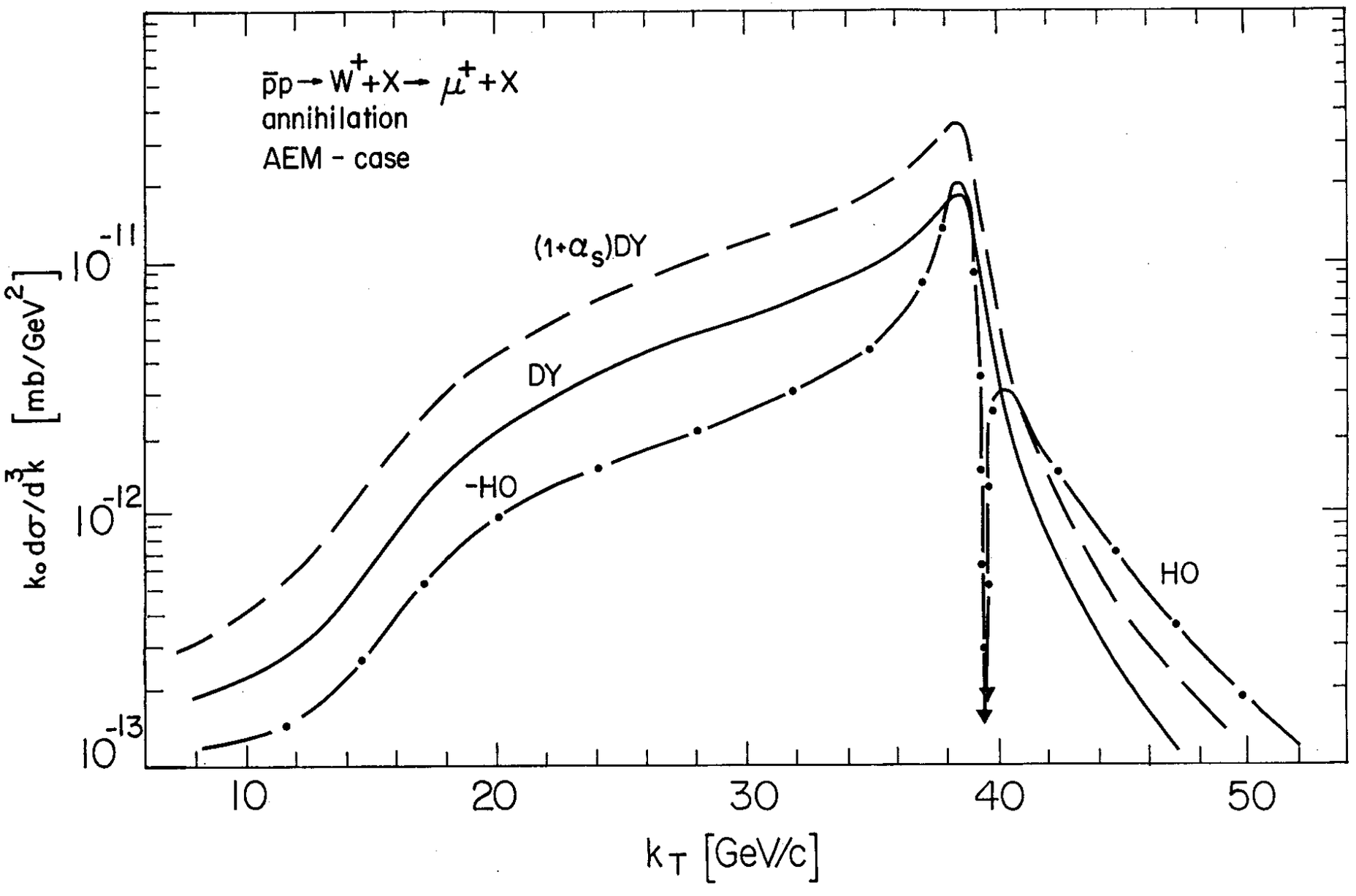
$\bar{p}p \to W^+ + X \to \mu^+ + X$
annihilation
AEM - case
$(1+\alpha_s)$DY
DY
-HO
HO
$k_o\, d\sigma/d^3k$ [mb/GeV^2]
10^{-11}
10^{-12}
10^{-13}
10
20
30
40
50
k_T [GeV/c]

FIG. 3b

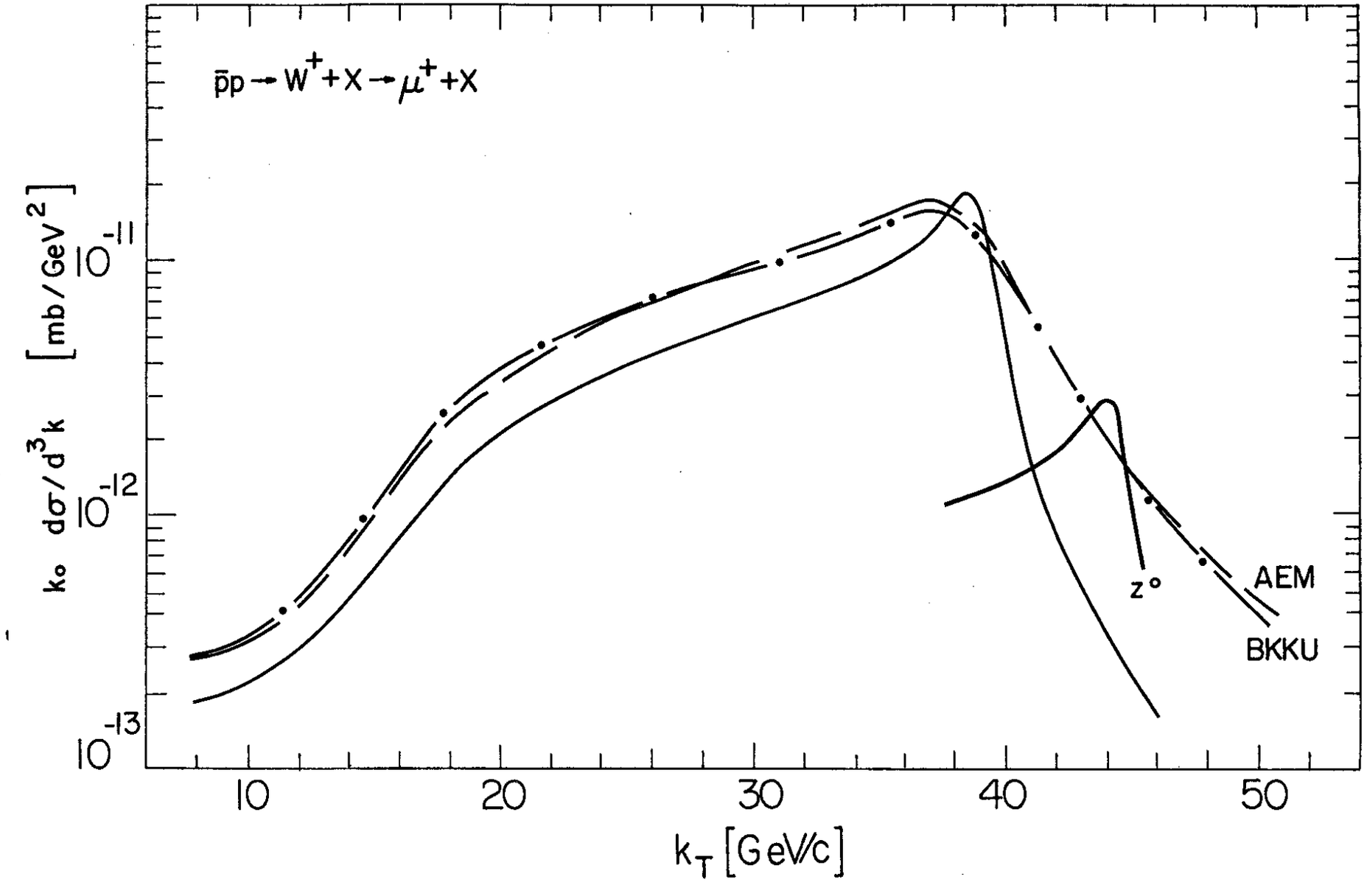
$\bar{p}p \rightarrow W^+ + X \rightarrow \mu^+ + X$
$k_o \, d\sigma/d^3k$ [mb/GeV^2]
10^{-11}
10^{-12}
10^{-13}
10
20
30
40
50
k_T [GeV/c]
z^o
AEM
BKKU

FIG. 4